Journal of Southeast University (English Edition) Vol. 38, No. 3, pp. 260 - 269 Sept. 2022 ISSN 1003—7985

Experimental study of pre-cracked concrete subjected to cryogenic freeze-thaw cycles based on an LNG concrete tank

Zhang Puyang[1] Ma Yuxuan[1] Liu Yang[2] Xu Yunlong[1] Ding Hongyan[1]

([1]State Key Laboratory of Hydraulic Engineering Simulation and Safety, Tianjin University, Tianjin 300072, China)
([2]CNOOC Petroleum and Gas Power Group Co., Ltd., Beijing 100020, China)

Abstract: To investigate the mechanical properties of concrete under the leakage condition for a liquefied natural gas storage tank, cryogenic freeze-thaw cycle tests were performed under liquid nitrogen refrigeration and water immersion melting. The effects of the cryogenic temperature, freeze-thaw cycle, pre-crack, and addition of steel fiber on the compressive strength, flexural strength, and splitting tensile concrete strength were analyzed. The experimental results show that the width of pre-cracks tends to expand after freeze-thaw cycles. When the freezing temperature is −80 ℃, the relative width of the pre-cracks expands by 1 to 2 times. However, when the freezing temperature is −120 ℃, the relative width of the pre-cracks expands by 2 to 5 times. Compared with the specimens without steel fibers, the specimens with steel fibers can still maintain a relatively complete appearance structure after the mechanical property tests. The compressive strength, flexural strength, and splitting tensile concrete strength decrease with the drop in the freezing temperature. After adding steel fibers, all of the three strengths increased.

Key words: cryogenic temperature; freeze-thaw cycle; pre-cracked concrete; steel fibers; mechanical properties
DOI: 10.3969/j.issn.1003-7985.2022.03.007

As emerging energy, liquefied natural gas (LNG) is safer, cleaner, more reliable, and more efficient than conventional energy. Furthermore, as an effective storage method, the demand for the construction of large-scale LNG storage tanks is increasing[1]. Existing large storage tanks are usually LNG full containment tanks[2], consisting of a metal inner tank and a concrete outer tank. There is also an insulating layer between the two tanks. At the standard atmospheric pressure, the boiling point of LNG is −162.15 ℃. If the inner tank is damaged, LNG leaks to the layer between two tanks, causing the exposure of the inner side of the outer concrete tank to a cryogenic temperature environment of approximately −102 ℃[3]. The huge temperature difference between the inside and outside of the concrete tank creates cryogenic freeze-thaw cycles, but the freeze-thaw resistance of concrete is poor[4]. If there are also cracks in the concrete tank, the damage caused by the freeze-thaw becomes severe, and the tank service life is further reduced. Therefore, how to reduce the weakening effect of cracks and cryogenic freeze-thaw cycles on the mechanical properties of concrete should be investigated.

For a long time, researchers have been exploring the effects of cracks on the performance of concrete. Many researchers have examined the principle of cracks in concrete and their effects on the mechanical properties of concrete by prefabricating cracks on concrete specimens. Pimamnas et al.[5] investigated the effects of existing cracks on the shear failure behavior of reinforced concrete members. Their results showed that a reduction in the effective contact area of the cracked surface and the corresponding reduction in the compressive concrete strength near the pre-crack are due to the micro-fracturing damages. Zhang et al.[6] found that most of the fracture parameters of a concrete composite are significantly influenced by the pre-crack length of beam specimens. Fu et al.[7] conducted an experimental work by introducing 0.5-mm- and 1.0-mm-wide pre-cracks in beam cross-sections and demonstrated that the section pre-cracks led to a significant shear strength degradation. Mousavi et al.[8] attempted to explain the bond failure mechanisms in pre-cracked concrete using a simplified theoretical model. However, the parameters of the freeze-thaw cycle were rarely considered, especially at cryogenic temperatures.

From the 1950s to the 1970s, the effects of cryogenic temperatures on the mechanical properties of concrete were studied in the United States, Japan, and other countries[9]. In recent years, Xie et al.[10-14] used liquid nitrogen to create a cryogenic temperature environment for concrete specimens. They conducted a series of experiments related to concrete under this environment, focusing on the mechanical property of prestressed concrete members and exploring the changes in the microstructure of concrete through a scanning electron microscope. For reference, the method presented above will be used for cryogenic temperature freeze-thaw cycles.

Previous studies show that the essence of concrete deterioration due to freeze-thaw cycles is that such cycles in-

Received 2021-12-16, **Revised** 2022-05-08.

Biography: Zhang Puyang (1978—), male, doctor, associate professor, zpy_td@163.com.

Citation: Zhang Puyang, Ma Yuxuan, Liu Yang, et al. Experimental study of pre-cracked concrete subjected to cryogenic freeze-thaw cycles based on an LNG concrete tank[J]. Journal of Southeast University (English Edition), 2022, 38(3): 260 - 269. DOI: 10.3969/j.issn.1003-7985.2022.03.007.

tensify the initial crack growth and induce the occurrence and development of new cracks[15-17]. However, after the fiber is added to concrete, it can carry part of the loads and alleviate the stress concentration issue at the internal defects of the concrete. Furthermore, the fiber that crosses the crack can still transmit stress and resist the external force[18].

To prevent or delay the damage to the outer tank, fibers can be added to concrete to strengthen and toughen the concrete matrix[19-22]. Fibers can be made of steel, glass, polypropylene, or basalt. At present, researchers mainly discuss the strengthening effect of fibers on concrete from the aspects of type, size, shape, dosage, and mixing[23-27]. Zhang et al.[28] proved that the compressive concrete strength with the proper amount of steel fiber is higher than that of ordinary concrete. Kachouh et al.[29] found that when the steel fiber content increased from 0% to 3%, the compressive concrete strength using recycled aggregates increased by 5.67% to 13.36%. Luo et al.[30] performed 500 routine freeze-thaw cycle tests and found that with the increase in the steel fiber content, the compressive strength and splitting tensile strength increased by about five and four times, respectively, and the mass-loss rate decreased by approximately 90%.

As a summary of earlier studies, the parameters of pre-crack, steel fiber, and freeze-thaw cycles on concrete have not been considered together. Thus, the present study mainly aims to identify the effects of steel fibers added to pre-crack concrete, which has been subjected to cryogenic freeze-thaw cycles. The specimens were repeatedly frozen at cryogenic temperatures and melted at 20 ℃. The resulting mechanical properties were determined by testing the cubic, prismatic, and cylindrical specimens. The test results provide a theoretical basis for the concrete structure design of LNG storage tanks.

1 Test Program

1.1 Design of the specimen and experiment scheme

According to the Standard for Test Methods of Concrete Physical and Mechanical Properties[31], cubic (150 mm side), prismatic (size 600 mm × 150 mm × 150 mm), and cylindrical concrete specimens (150 mm × 300 mm) were fabricated. After being subjected to cryogenic freeze-thaw cycles, the compressive strength, flexural strength, and splitting tensile strength of the concrete specimens were tested. The design concrete strength in this experiment was C50. Moreover, steel fiber was added to some of the concrete specimens, and the mass ratio of steel fiber to cement was 1∶5. The water-cement ratio was 9∶25. Moreover, the length of steel fiber was 35 to 40 mm, and its width was 0.3 to 0.9 mm.

Based on the Standard for Test Methods of Long-term Performance and Durability of Ordinary Concrete[32], the scheme for the experiment was drawn up. The freezing temperatures (determined as −80 and −120 ℃ in the environment temperature of the LNG leak and the effective constant temperature capacity of the incubator) and the width of pre-cracks (i.e., 0.1 and 0.2 mm) were taken as testing variables for plain concrete and fiber-reinforced concrete specimens. The specimens were subjected to five cycles of cryogenic temperature freezing and thawing. The specimens of each shape were divided into five groups. Each group contained three specimens. The total number of specimens was therefore 45. The naming format of the groups for specimens is the shape number-sequence number. The shape numbers A, B, and C represent the cube, prism, and cylinder, respectively. The design of the specimens is shown in Tab. 1.

Tab. 1 Design of the concrete specimens

Group No.	Temperature/℃	Width of Pre-crack/mm	Whether it contains steel fiber
A-1	20	0.1	Negative
A-2	−80	0.1	Negative
A-3	−120	0.1	Negative
A-4	−80	0.1	Positive
A-5	−80	0.2	Negative
B-1	20	0.1	Negative
B-2	−80	0.1	Negative
B-3	−120	0.1	Negative
B-4	−80	0.1	Positive
B-5	−80	0.2	Negative
C-1	20	0.1	Negative
C-2	−80	0.1	Negative
C-3	−120	0.1	Negative
C-4	−80	0.1	Positive
C-5	−80	0.2	Negative

1.2 Experiment equipment

In this experimental study, air freezing and water thawing methods were used to perform the cryogenic freeze-thaw cycles. The experimental device includes three parts: a cryogenic temperature freezing device, a water tank, and a temperature measurement system. Moreover, as shown in Fig. 1(a), the cryogenic temperature freezing device includes a liquid nitrogen storage tank and polyurethane incubator. The water tank used to thaw the specimen is shown in Fig. 1(b). The temperature measurement system includes the reading device LU-906M regulator (see Fig. 1(c)) and the cryogenic temperature sensor. The lowest temperature in the incubator can be reduced to −170 ℃, and the freezing rate of the specimen can be controlled by manually adjusting the release rate of liquid nitrogen. The low temperature measurement limit of the cryogenic temperature sensor placed inside the incubator/water box and specimen is −200 ℃. Furthermore, the reading device is used to monitor the temperature by connecting with the sensor. As shown in Fig. 1(d), the crack width was measured by the crack width instrument, which is a high-definition magnifying

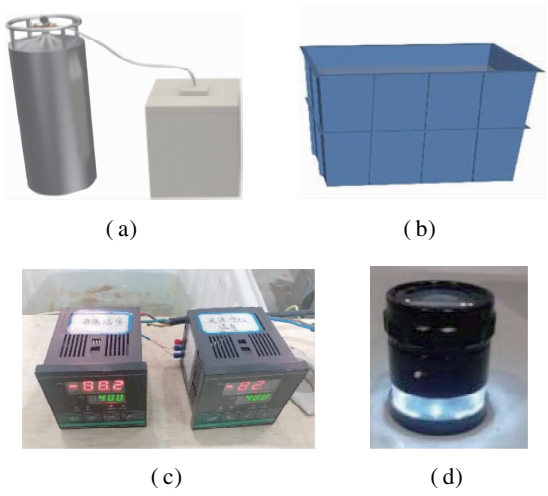

(a) (b) (c) (d)

Fig. 1 Set of test equipment for subjecting the concrete specimens to cryogenic freeze-thaw cycles. (a) Liquid nitrogen Dewar flask and polyurethane incubator; (b) Water tank for restoring specimens to 20 ℃; (c) LU-906M intelligent regulator; (d) Crack width measuring instrument

glass with a cross reticle. The maximum measuring range of the instrument is 30 mm, and the minimum is 0.1 mm.

After the object mirror was placed on the crack, the eyepiece focal length was adjusted to make the observation clear. In this way, the crack width can be measured by the cross reticle mark. As shown in Fig. 2, the stainless steel sheet was used to create a pre-crack in each specimen. Therefore, in this study, four different sizes of high-strength and high-toughness sheets were produced. In terms of length, width, and thickness, their sizes are 150 mm × 70 mm × 0.1 mm, 150 mm × 70 mm × 0.2 mm, 200 mm × 70 mm × 0.1 mm, and 200 mm × 70 mm × 0.2 mm, respectively. The first two sizes of sheets were used to prefabricate the cracks in the cubic and prismatic specimens, and the latter two sizes of sheets were used to prefabricate the cracks in the cylindrical specimens. As shown in Fig. 2, in the manufacturing process, the sheet was inserted into the concrete to be hardened by 63 mm. This insertion depth was determined from the statistical analysis of a certain storage tank crack detection. Then, the sheet was removed after the concrete was initially set. The different width cracks were obtained by inserting different size sheets.

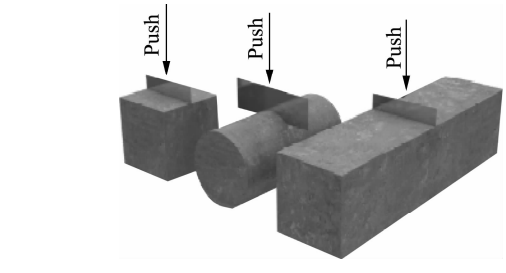

Fig. 2 Manufacture of pre-cracks inthe concrete specimens

1.3 Control of temperature regulation

To effectively control the freezing and thawing of the concrete specimens, the specimens were frozen at −120 ℃ and subsequently thawed. The arrangements of the specimens in the incubator and water tank are shown in Figs. 3 and 4, respectively. As shown in Fig. 4, the spacing between the specimens was increased as much as possible to ensure their complete contact with water while immersing them in the water tank. As shown in Fig. 4, when the specimens were placed in the incubator, the spacing should be kept minimum to maintain their constant temperature. However, the specimens must not be in contact with one another, or else they will stick together. To reduce the influence of the size effect on the experiment, the freezing method was used in advance on the large specimens. In other words, the order of putting the specimens into the incubator is according to the size. That is, the prismatic specimens were put first, followed by the cylindrical and cubic specimens. Before the next specimen was placed into the incubator, the previous size specimen was already frozen, so there was a temperature difference of 15 and 20 ℃. After the cubic specimens were placed into the incubator, data collection was started, and the freezing rate was maintained at 0.5 to 1.5 ℃/min. In Fig. 5, t refers to the time of the test. The order of the specimens to reach the freezing temperature is the prismatic specimen, then the cylindrical specimen, and finally the cubic specimen. After reaching the freezing temperature, all the specimens were kept at this

Fig. 3 Arrangement of the concrete specimens inside the water tank

Fig. 4 Arrangement of the concrete specimens inside the incubator

temperature for 4 h to ensure the uniform temperature inside the specimens. The freezing and subsequent temperature holding lasted for approximately 360 min. At the end of the freezing and temperature holding, the concrete specimens were quickly soaked in water for thawing, and the water surface was at least 20 mm above the upper surface of the specimens. The specimens thawed quickly inside the water, and the specimens' temperature rose from −120 to 20 ℃ in only approximately 96 min.

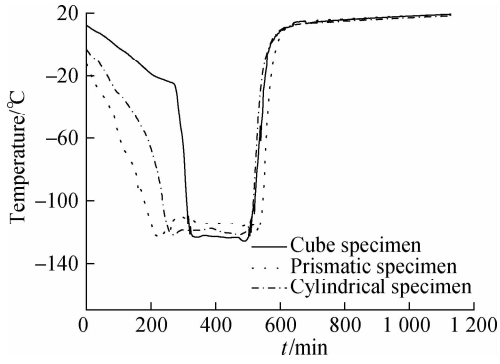

Fig. 5 Temperature of concrete specimens during a freeze and thaw cycle

2 Test Results and Discussions

2.1 Phenomena of experimental results

After freezing and holding the freezing temperature, the specimens were taken out of the incubator. As shown in Fig. 6(a), the surface was covered with a layer of white frost. When the frost was removed with a fine bristle brush, there was no noticeable change. When the specimen was placed into the water tank, the white frost quickly disappeared. After thawing and holding the thawing temperature, the specimens were removed from the water tank. Then, the water on the surface was gently wiped so that fine cracks could be seen. Overall, the appearance of the specimens can be inspected after every freeze-thaw cycle as described above. As shown in Fig. 6(b), the mortar on the surface of the specimen fell off in the form of debris. Furthermore, with the increase in the number of freeze-thaw cycles, the bubbles like pores with a size of fine aggregates gradually appeared on the specimen surface, as shown in Fig. 6(c). At the same time, different phenomena were observed on the surface of the specimens, such as the different degrees of cracks, missing edges and corners, exposed aggregates, and spalling of surface concrete mortar. Fig. 6(d) shows that several temperature cracks with different lengths can be seen after brushing off the fallen mortar and observing the cracks using the crack width meter. Their number is the highest, especially near the pre-cracks. With the increase in the number of freeze-thaw cycles, the degree of the surface mortar spalling becomes more severe. Furthermore, the thickness of the surface mortar peeling off of some specimens can reach 2 mm after the fifth freeze-thaw cycle. The number of temperature cracks under the chippings of peeling mortar also increased exponentially.

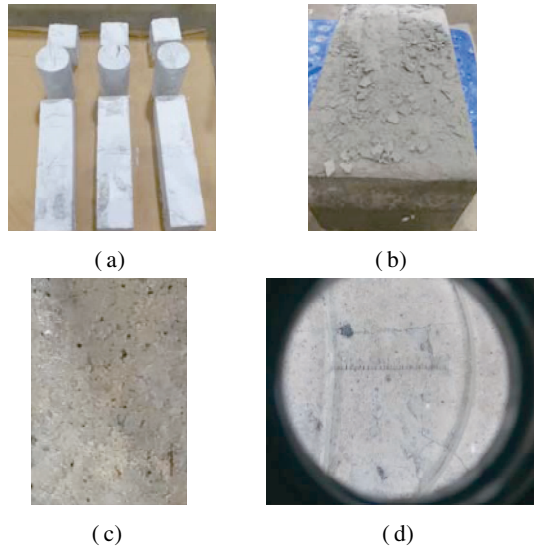

Fig. 6 Experimental phenomena of the concrete specimens after freezing or thawing. (a) Concrete specimens after freezing; (b) Concrete specimens after thawing; (c) Some small bubble-shaped hole; (d) Fine cracks under the width measuring instrument

The results of the pre-crack width are shown in Tab. 2. The pre-crack widths were measured at the design depth of the pre-crack (i.e., 63 mm) on the side of the specimens. In this study, the side of the sheet was inserted as the bottom of the specimen. The reason is that when the sheet was inserted, the steel fibers of the concrete, which were initially located in the area of the pre-crack, were squeezed apart. In addition, the primary purpose of adding steel fibers is to prevent the extension of pre-cracks. As the change in the pre-crack width is discrete, the widths of the pre-cracks are given in Tab. 2, which are the average width of the specimens in each group, taken to one decimal place.

Tab. 2 Width of pre-cracks after five freeze-thaw cycles

Group No.	A-1	A-2	A-3	A-4	A-5	B-1	B-2	B-3	B-4	B-5	C-1	C-2	C-3	C-4	C-5
Width/mm	0.1	0.2	0.1	0.1	0.4	0.1	0.3	0.1	0.3	0.5	0.2	0.3	0.2	0.2	0.4

To compare the variation of the pre-crack width intuitively, the data in Tab. 2 were made dimensionless; i.e., the changed crack width was divided by the corresponding pre-crack width giving a corresponding relative width of the pre-crack. In this way, the relative width of the pre-crack reflects the width change of the pre-crack.

If the relative width of the pre-crack is unified, there is no change in the pre-crack width after five freeze-thaw cycles. However, if the relative width of the pre-crack is a constant greater than one, the pre-crack width increases by the constant multiple after five freeze-thaw cycles. In Fig. 7, θ refers to the centigrade degree of the freezing temperature. With the decrease in the freezing temperature, the relative width of the pre-cracks of all the three specimens increases; i. e., the lower the freezing temperature, the wider the pre-crack. Moreover, when the freezing temperature was −120 ℃, the maximum relative width of the pre-cracks could reach 5. On the one hand, taking the relative width of the pre-cracks at 20 ℃ as a reference, the relative width of the pre-cracks increased by 1 to 2 times when the freezing temperature was −80 ℃, and the relative width of the pre-cracks increased by 2 to 5 times when the freezing temperature was −120 ℃. Compared with the relative width of the pre-cracks when the freezing temperature was −80 ℃, the relative width of the pre-cracks increased by 0.33 to 0.67 times when the freezing temperature was −120 ℃. The variation trend of the relative width of the pre-cracks of the three specimens is inconsistent, which may be attributed to the nonuniform freezing caused by the shape effect of the specimens. Furthermore, as shown in Fig. 8, steel fibers restricted the increase in the relative width of pre-cracks. In conclusion, compared to the relative width of pre-cracks of concrete without steel fibers, the relative width of the pre-cracks of concrete with steel fibers is shortened by 1 to 2. In particular, for the prismatic specimens with the designed pre-crack width of 0.1 mm, the relative widths are the same for the specimens with and without steel fibers. This outcome can be attributed to the large volume of the prismatic specimens, uneven distribution of steel fibers, and fewer fiber distributed near the pre-cracks.

As shown in Fig. 8, the inserted side of the sheet is the bottom surface of the specimen, whereas the opposite side is the top surface. During the compressive strength testing

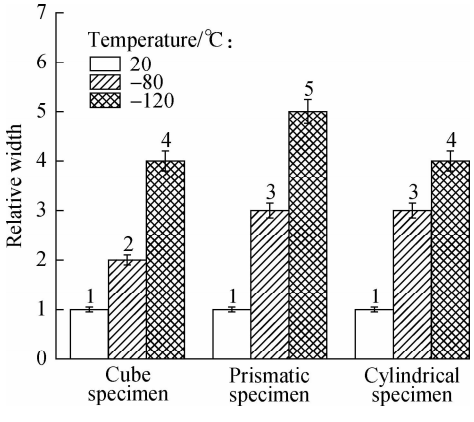

Fig. 7 Effect of the cryogenic temperature on the relative width of the pre-cracks

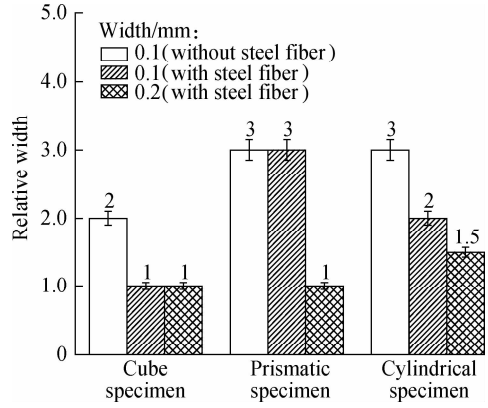

Fig. 8 Effects of steel fibers and pre-crack width on the variation of the crack width

of the concrete specimen, the top of the specimen was taken as the loading surface. The process of the mechanical property testing on the specimens of the three different shapes is similar. However, there are some differences, which will be discussed later. Therefore, only the cubic specimen was taken as an example to explain the test process. The compressive strength test of a concrete specimen after the cryogenic freeze-thaw cycles mainly includes the following processes:

1) At the beginning, when a load is applied to the specimen, the load-time curve on the monitor of the concrete pressure testing machine linearly increases, and there is no apparent physical change in the specimen.

2) When the load is about to reach the ultimate load, micro-cracks appear on the specimen surface along the loading direction, and the surface starts chipping and falling off.

3) The sharp drop in the load-time curve indicates that the specimen loses its strength and is completely destroyed with a loud, dull noise.

Under the loading by the concrete testing machine, as shown in Fig. 9(a), for the specimen without steel fibers, a few fragments fell off. At the same time, the pre-cracks rapidly progressed until they penetrated the specimen. Furthermore, the specimen was taken out for careful observation, as shown in Fig. 9(b). The primary failure mode was observed as a splitting failure. As shown in Fig. 9(c), the specimen can be easily separated by hand along the pre-crack direction. The failure surface along the pre-crack was relatively flat, and there were no irregular pits and bulges. Moreover, there was no aggregate adhesion, and its color was dark cyan. As shown in Fig. 9(d), for the specimen with steel fibers, there was no large fragment falling off, and only the concrete surface bulged out. The main reason for the splitting failure is that the pre-cracks of the specimen extended to the specimen's top after the freeze-thaw cycles, but the steel fiber limited the progression.

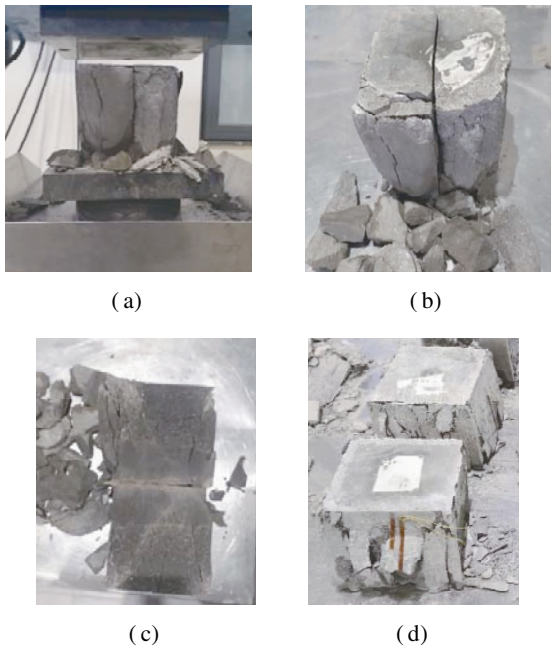

(a) (b) (c) (d)

Fig. 9 Failure modes of a cubic concrete specimen. (a) Failure mode of cleavage; (b) Failure mode of crush; (c) Fracture surface of the cleavage; (d) Failure mode of the specimen with steel fibers

The failure mechanism of the prism flexural strength test and cylinder splitting tensile strength test is somewhat similar to that of the cube compressive strength test, as discussed above. However, there are some different characteristics. For the prismatic specimen, with the press loading, the pre-crack of the prismatic specimen spread to the top surface from the side view, as shown in Fig. 10(a).

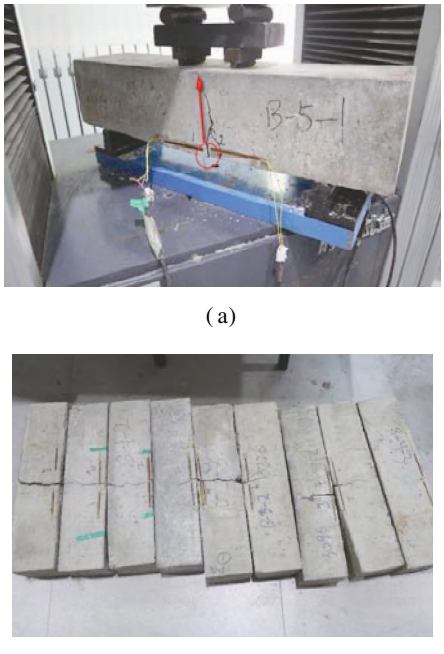

(a) (b)

Fig. 10 Failure modes of the prismatic concrete specimen. (a) Crack development during loading onto the specimen; (b) Prismatic concrete specimen after failure

The appearance of the prismatic specimen after a complete failure is shown in Fig. 10(b), and all of them failed at the pre-crack location. In the splitting tensile strength test, micro-cracks can be seen on the circular periphery of the cylinder specimen, which slowly extends from the bottom to the top. With a dull sound, the specimen lost its strength. Due to the existence of pre-cracks, most specimens were split into four parts, as shown in Fig. 11.

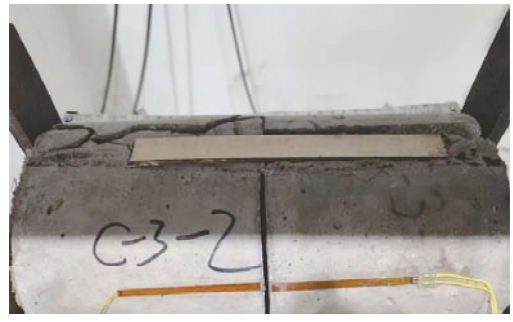

Fig. 11 Failure mode of the cylindrical concrete specimen

2.2 Effect of the temperature range on the strength of pre-cracked concrete

Fig. 12 shows the average compressive, flexural, and splitting tensile strength values of three specimens in each group. Overall, the compressive concrete strength is still much greater than the tensile and flexural strengths after five cryogenic freeze-thaw cycles. The first group is the control group tested at 20 ℃. The freezing temperatures of the second and third groups are −80 and −120 ℃, respectively. The pre-crack width of all these specimens is 0.1 mm. For the three groups of cubic specimens, the compressive strengths of Groups A-1, A-2, and A-3 are 48.1, 43.3, and 30.6 MPa, respectively. Thus, it can be inferred that the lower the freezing temperature, the more significant the weakening effect on the concrete cube's compressive strength. In addition, the compressive strength of Group A-2 is 9.98% lower than that of Group A-1, whereas that of Group A-3 is 36.38% lower than that of Group A-1. Compared with Group A-2, the compressive strength of Group A-3 is 29.33% lower.

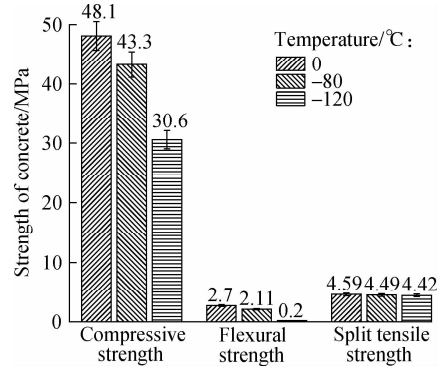

Fig. 12 Effect of the cryogenic temperature on the concrete strength

For the three groups of prismatic specimens, the flexural concrete strength in Groups B-1, B-2, and B-3 are 2.7, 2.11, and 0.2 MPa, respectively. The lower the freezing temperature, the more significant the weakening effect on the flexural strength of the prismatic specimens. In addition, the flexural strength of Group B-2 is 21.85% lower than that of Group B-1, whereas that of Group B-3 is 92.59% lower than that of Group B-1. In addition, the flexural strength of Group B-3 is 90.52% lower than that of Group B-2. The sudden loss in flexural strength occurred at −120 ℃ due to the rapid extension of the pre-cracks. In Group B-3, after only three freeze-thaw cycles, some specimens were frozen to fracture; i.e., the prismatic specimens were broken along the pre-crack. However, even though the cylindrical and cubic specimens were frozen in the same incubator, they did not suffer such fractures. This outcome can be attributed to the higher temperature transfer rate of the cubic and cylindrical specimens as compared with the prismatic specimens. Therefore, their internal and external temperature differences and temperature stresses are small.

For the three groups of cylindrical specimens, the splitting tensile strength of Groups C-1, C-2, and C-3 are 4.59, 4.49, and 4.42 MPa, respectively. The lower the freezing temperature, the weaker the splitting tensile strength. In addition, the flexural strength of Groups C-2 and C-3 is 2.2% and 3.70% lower than that of Group C-1, respectively, whereas the flexural strength of Group C-3 is 1.56% lower than that of Group C-2.

Furthermore, the strength of the concrete subjected to cryogenic freeze-thaw cycles was divided by the strength of the corresponding room control temperature to obtain the dimensionless quantity, i.e., the relative strength, as shown in Fig. 13. The relative splitting tensile concrete strength decreases the least, whereas the relative flexural strength has the highest decrease, followed by the relative compressive strength. As the freezing temperature decreased, the relative splitting tensile strength linearly changed. However, the relative compressive and relative flexural strengths nonlinearly changed, i.e., the lower the freezing temperature, the greater the decrease in the relative compressive and relative flexural strengths.

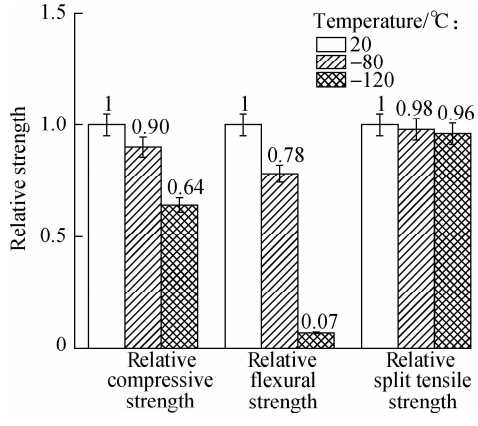

Fig. 13 Effect of the cryogenic temperature on the relative strength

During freezing, the pore water in the concrete accumulated in the pre-crack. The water froze and expanded, producing frost heaving pressure and increasing the number of pores. Hence, cracks grew. After repeated freeze-thaw cycles, the internal damage and prefabricated concrete defects gradually accumulated, making the structure weak. In addition, the accumulation of internal damage and prefabricated defects weakened the flexural strength the most, followed by the compressive strength.

2.3 Effect of steel fibers on the pre-cracked concrete strength

The effects of steel fibers and precast crack width on the strength of the concrete specimens are discussed in this section. Fig. 14 shows the average strength of the specimens in the group. All the specimens were subjected to cryogenic freeze-thaw cycles with a freezing temperature of −80 ℃. For the three types of specimens, the pre-crack width of the second group is 0.1 mm without steel fibers, whereas that of the fourth group is 0.1 mm with steel fibers. Steel fibers were added to the concrete specimens in the fifth group with a pre-crack width of 0.2 mm. As shown in Fig. 14, the compressive strength of Groups A-2, A-4, and A-5 is 43.3, 57.4, and 52.7 MPa, respectively. The compressive strength of Group A-4 is 32.6% higher than that of Group A-2. The compressive strength of Group A-5 is 21.7% higher than that of Group A-2, whereas the compressive strength of Group A-5 is 8.19% lower than that of Group A-4. The compressive strength of the specimens with steel fibers is higher than those without steel fibers. The strengthening effect of steel fibers on the compressive concrete strength is more pronounced than the weakening effect induced due to the large pre-crack width.

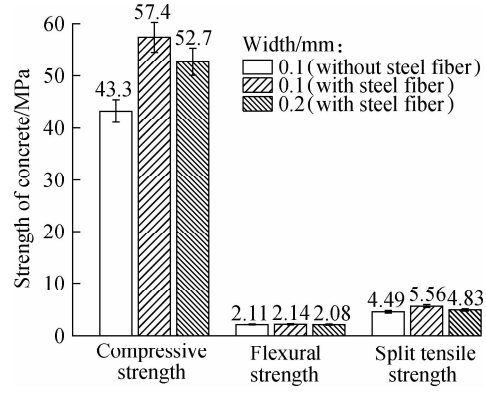

Fig. 14 Effects of steel fibers and pre-crack width on the concrete strength

For the prismatic specimens, the flexural strength of Groups B-2, B-4, and B-5 are 2.11, 2.14, and 2.08 MPa, respectively. The flexural strength of Group B-4 is

1.42% higher than that of Group B-2, whereas that of Group B-5 is 1.42% lower than that of Group B-2. The flexural strength of Group B-5 is 1.42% lower than that of Group B-2, whereas that of Group B-5 is 2.80% lower than that of Group B-4. After being subjected to the freeze-thaw cycles, steel fibers increased the concrete flexural strength. However, the increased strength was offset as the width of the pre-crack increased, which shows that the crack width has a significant impact on the concrete flexural strength.

For the cylindrical specimens, the splitting tensile strength of Groups C-2, C-4, and C-5 is 4.48, 4.65, and 4.51 MPa, respectively. The splitting tensile strength of Groups C-4 and C-5 is 3.79% and 0.67%, respectively, higher than that of Group C-2. The splitting tensile strength of Group C-5 is 3.01% lower than that of Group C-4. After being subjected to the cryogenic freeze-thaw cycles, the enhancement effect of steel fiber on the splitting tensile concrete strength is greater than the weakening effect induced due to pre-cracks on the compressive strength of the concrete cylinder. However, as the width of the pre-crack increased, there was a slight decrease in the enhancement effect.

To facilitate a fair analysis and comparison, a dimensionless analysis should be performed. Dividing the strength of the concrete after the cryogenic freeze-thaw cycles by the strength of the corresponding specimen without steel fibers gives the relative concrete strength, as shown in Fig. 15. The addition of steel fibers to the concrete has the most significant strengthening effect on the relative compressive concrete strength. However, the strengthening effect on the relative flexural concrete strength was not apparent, whereas that on the relative splitting tensile concrete strength was somewhere between the two. For the concrete specimens with steel fibers, the crack width significantly affected the relative splitting tensile strength. However, it has a negligible effect on the relative compressive and flexural strengths.

The added steel fibers to the concrete can firmly bond

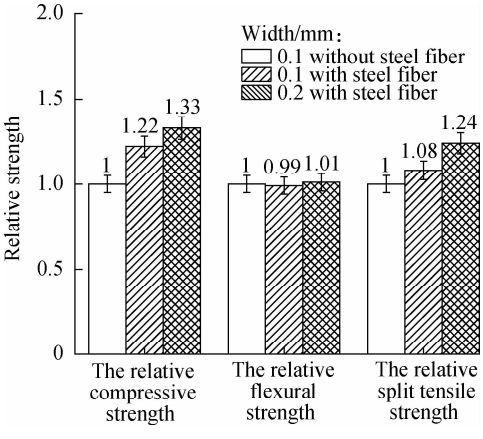

Fig. 15 Effects of steel fiber and pre-crack widths on the relative concrete strength

with the concrete matrix, even though its distribution in the concrete is nonuniform. Nonetheless, it makes the concrete compact and improves the concrete toughness. Therefore, steel fiber-reinforced concrete can effectively inhibit the growth of micro-cracks and limit the further development of pre-cracks.

3 Conclusions

1) In this study, a mechanical strength test was conducted after subjecting the specimens to the freeze-thaw cycles. The results show that the failure mode of the specimens with steel fibers was broken but not scattered as compared with the concrete specimens without steel fibers.

2) With the decrease in the freezing temperature, the designed pre-crack width of the specimens widened after the freeze-thaw cycles. Compared with the control group at 20 ℃, the relative width of the pre-cracks subjected to five freeze-thaw cycles at −80 ℃ increased by 1 to 2 times, and the relative width of the pre-cracks increased by 2 to 5 times when the freezing temperature was −120 ℃. Taking the relative width of the pre-cracks at −80 ℃ as a reference, the relative width of the pre-cracks at −120 ℃ increased by 0.33 to 0.67 times after five freeze-thaw cycles.

3) The compressive strength, flexural strength, and splitting tensile concrete strengths decreased with decreasing freezing temperature. In addition, the decrease in the flexural strength is the largest, followed by the compressive strength and then the splitting tensile strength. As another critical weakening property testing variable, the increase in the pre-crack width on the specimen weakened the concrete strength, just like the effect of the freeze-thaw cycle.

4) The mechanical properties of the specimen were tested after the cryogenic freeze-thaw cycles. The compressive strength, flexural strength, and splitting tensile strength were improved by adding steel fibers to the concrete. With the increase in the designed pre-crack width, the strengthening effect of steel fiber on concrete strength was weakened.

References

[1] Yan J B, Xie J, Behaviours of reinforced concrete beams under low temperatures [J]. *Construction and Building Materials*, 2017, **141**: 410 − 425. DOI: 10.1016/j.conbuildmat.2017.03.029.

[2] Jiang Z W, Zhang C, Deng Z L, et al. Thermal strain of cement-based materials under cryogenic temperatures and its freeze-thaw cycles using fiber Bragg grating sensor [J]. *Cryogenics*, 2019, **100**: 1 − 10. DOI: 10.1016/j.cryogenics.2019.03.005.

[3] Xie J, Cui N, Yan J B, et al. Experimental study on prestress losses of post-tensioned concrete members at ultra-low temperatures [J]. *Structural Concrete*, 2019, **20**(6):

1828 − 1841. DOI: 10. 1002/suco. 201800264.

[4] Dong Y J, Su C, Qiao P Z, et al. Microstructural damage evolution and its effect on fracture behavior of concrete subjected to freeze-thaw cycles [J]. *International Journal of Damage Mechanics*, 2018, **27**(8): 1272 − 1288. DOI: 10. 1177/1056789518787025.

[5] Pimamnas A, Tisavipat J. Effect of existing cracks on shear failure behaviour of reinforced concrete members [J]. *Magazine of Concrete Research*, 2005, **57**(8): 485 − 495. DOI: 10. 1680/macr. 2005. 57. 8. 485.

[6] Zhang P, Gao J X, Zhu H T, et al. Effect of prefabricated crack length on fracture toughness and fracture energy of fly ash concrete reinforced by nano-SiO_2 and fibers [J]. *Iranian Journal of Science and Technology—Transactions of Civil Engineering*, 2016, **40**(1): 69 − 74. DOI: 10. 1007/s40996-016 − 0013-4.

[7] Fu L, Nakamura H, Yamamoto Y, et al. Investigation of influence of section pre-crack on shear strength and shear resistance mechanism of RC beams by experiment and 3-D RBSM analysis [J]. *Journal of Advanced Concrete Technology*, 2017, **15**(11): 700 − 712. DOI: 10. 3151/jact. 15. 700.

[8] Mousavi S S, Guizani L, Ouellet-Plamondon C M. Simplified analytical model for interfacial bond strength of deformed steel rebars embedded in pre-cracked concrete [J]. *Journal of Structural Engineering*, 2020, **146**(8): 04020142. DOI: 10. 1061/(ASCE) ST. 1943-541X. 0002687.

[9] Xie J, Li X M, Wu H H, Experimental study on the axial-compression performance of concrete at cryogenic temperatures [J]. *Construction and Building Materials*, 2014, **72**: 380 − 388. DOI: 10. 1016/j. conbuildmat. 2014. 09. 033.

[10] Xie J, Kang E C, Yan J B, et al. Pull-out behaviour of headed studs embedded in normal weight concrete at low temperatures [J]. *Construction and Building Materials*, 2020, **264**: 120692. DOI: 10. 1016/j. conbuildmat. 2020. 120692.

[11] Xie J, Cui N, Yan J B, et al. Experimental study on prestress losses of post-tensioned concrete members at ultra-low temperatures [J]. *Structural Concrete*, 2019, **20**(6): 1828 − 1841. DOI: 10. 1002/suco. 201800264.

[12] Xie J, Yan J B, Experimental studies and analysis on compressive strength of normal-weight concrete at low temperatures [J]. *Structural Concrete*, 2018, **19**(4): 1235 − 1244. DOI: 10. 1002/suco. 201700009.

[13] Xie J, Zhao X Q, Yan J B, Experimental and numerical studies on bonded prestressed concrete beams at low temperatures [J]. *Construction and Building Materials*, 2018, **188**: 101 − 118. DOI: 10. 1016/j. conbuildmat. 2018. 08. 117.

[14] Xie J, Chen X, Yan J B, et al. Ultimate strength behavior of prestressed concrete beams at cryogenic temperatures [J]. *Materials and Structures*, 2017, **50**(1): 1 − 13. DOI: 10. 1617/s11527-016 − 0956-8.

[15] Dahmani L, Khenane A, Kaci S, Behavior of the reinforced concrete at cryogenic temperatures [J]. *Cryogenics*, 2007, **47**(9/10): 517 − 525. DOI: 10. 1016/j. cryogenics. 2007. 07. 001.

[16] Jiang Z W, He B, Zhu X P, et al. State-of-the-art review on properties evolution and deterioration mechanism of concrete at cryogenic temperature [J]. *Construction and Building Materials*, 2020, **257**: 119456. DOI: 10. 1016/j. conbuildmat. 2020. 119456.

[17] Luo Y J, Cui W, Song H F. Poromechanical microplane model with thermodynamics for deterioration of concrete subjected to freeze-thaw cycles [J]. *Journal of Materials in Civil Engineering*, 2020, **32**(11): 04020338. DOI: 0402033810. 1061/(Asce) Mt. 1943 − 5533. 0003438.

[18] Johannesson B. Dimensional and ice content changes of hardened concrete at different freezing and thawing temperatures[J]. *Cement and Concrete Composites*, 2010, **32**(1): 73 − 83. DOI: 10. 1016/j. cemconcomp. 2009. 09. 001.

[19] Kim M J, Kim S, Lee S K, et al. Mechanical properties of ultra-high-performance fiber-reinforced concrete at cryogenic temperatures [J]. *Construction and Building Materials*, 2017, **157**: 498 − 508. DOI: 10. 1016/j. conbuildmat. 2017. 09. 099.

[20] Song P S, Hwang S, Sheu B C. Strength properties of nylon-and polypropylene-fiber-reinforced concretes [J]. *Cement and Concrete Research*, 2005, **35**(8): 1546 − 1550. DOI: 10. 1016/j. cemconres. 2004. 06. 033.

[21] Nili M, Azarioon A, Danesh A, et al. Experimental study and modeling of fiber volume effects on frost resistance of fiber reinforced concrete [J]. *International Journal of Civil Engineering*, 2018, **16**(3): 263 − 272. DOI: 10. 1007/s40999-016 − 0122-2.

[22] Mansouri I, Shahheidari F S, Hashemi S M A, et al. Investigation of steel fiber effects on concrete abrasion resistance [J]. *Advances in concrete construction*, 2020, **9**(4): 367 − 374. DOI: 10. 12989/acc. 2020. 9. 4. 367.

[23] Kim M J, Yoo D Y, Kim S, et al. Effects of fiber geometry and cryogenic condition on mechanical properties of ultra-high-performance fiber-reinforced concrete [J]. *Cement and Concrete Research*, 2018, **107**: 30 − 40. DOI: 10. 1016/j. cemconres. 2018. 02. 003.

[24] Li J Q, Wu Z M, Shi C J, et al. Durability of ultra-high performance concrete—A review [J]. *Construction and Building Materials*, 2020, **255**: 119296. DOI: 11929610. 1016/j. conbuildmat. 2020. 119296.

[25] Kim M J, Yoo D Y. Analysis on enhanced pullout resistance of steel fibers in ultra-high performance concrete under cryogenic condition [J]. *Construction and Building Materials*, 2020, **251**: 118953. DOI: 10. 1016/j. conbuildmat. 2020. 118953.

[26] Kim M J, Kim S, Lee S K, et al. Mechanical properties of ultra-high-performance fiber-reinforced concrete at cryogenic temperatures [J]. *Construction and Building Materials*, 2017, **157**: 498 − 508. DOI: 10. 1016/j. conbuildmat. 2017. 09. 099.

[27] Wang Z H, Li L, Zhang Y X, et al. Bond-slip model considering freeze-thaw damage effect of concrete and its application [J]. *Engineering Structures*, 2019, **201**: 109831. DOI: 10. 1016/j. engstruct. 2019. 109831.

[28] Zhang P, Yang Y H, Wang J, et al. Mechanical properties and durability of polypropylene and steel fiber-reinforced recycled aggregates concrete (FRRAC): A review [J]. *Sustainability*, 2020, **12**(22): 9509. DOI: 10. 3390/su12229509.

[29] Kachouh N, El-Hassan H, EI-Maaddawy T. Effect of steel fibers on the performance of concrete made with recycled concrete aggregates and dune sand [J]. *Construction and Building Materials*, 2019, **213**: 348 – 359. DOI: 10.1016/j.conbuildmat.2019.04.087.

[30] Luo D M, Wang Y, Niu D T, Evaluation of the performance degradation of hybrid steel-polypropylene fiber reinforced concrete under freezing-thawing conditions [J]. *Advances in Civil Engineering*, 2020, **2020**: 8863047. DOI: 10.1155/2020/8863047.

[31] Ministry of Construction of the People's Republic of China. Standard for test methods of concrete physical and mechanical properties: GB/T 50081—2019 [S]. Beijing: China Architecture & Building Press, 2019. (in Chinese)

[32] Ministry of Construction of the People's Republic of China. Standard for test methods of long-term performance and durability of ordinary concrete: GB/T 50082—2009 [S]. Beijing: China Architecture & Building Press, 2009. (in Chinese)

基于 LNG 混凝土储罐的预制裂缝混凝土超低温冻融循环试验研究

张浦阳[1] 马宇轩[1] 刘 洋[2] 许云龙[1] 丁红岩[1]

([1] 天津大学水利工程仿真与安全国家重点实验室, 天津 300072)

([2] 中海石油气电集团有限公司, 北京 100020)

摘要: 为探究液化天然气混凝土储罐泄露工况下混凝土的物理力学特性,采用液氮制冷和浸水融化的方式,开展了混凝土超低温冻融循环试验,分析了超低温、冻融循环、预制裂缝、是否掺加钢纤维等因素对混凝土抗压强度、抗折强度、劈裂抗拉强度的影响. 试验结果表明,预制裂缝宽度在冻融循环后呈扩大趋势. 当冷冻温度为 –80 ℃时,预制裂缝相对宽度扩大 1 ~ 2 倍;当冷冻温度为 –120 ℃时,预制裂缝相对宽度扩大 2 ~ 5 倍. 与未掺加钢纤维的混凝土试件相比,掺有钢纤维的混凝土试件经历力学性能试验后仍能保持较完整的外观结构. 混凝土抗压强度、抗折强度、劈裂抗拉强度随冷冻温度降低而减小,掺加钢纤维后则均有所提高.

关键词: 超低温;冻融循环;预制裂缝混凝土;钢纤维;力学性能

中图分类号: TU528.1